

# Surface Protection and Morphological Study of Copper by Green Corrosion Inhibitor: 8QSC in HNO<sub>3</sub> Medium

R. Ganapathi Sundaram · M. Thamaraiselvi · G. Vengatesh ·  
M. Sundaravadivelu

Submitted: 23 February 2018 / in revised form: 13 April 2018 / Published online: 20 June 2018  
© ASM International 2018

**Abstract** The inhibition performance and surface protection of green corrosion inhibitor 8-quinoline sulphonyl chloride (8QSC) on copper (Cu) was evaluated by chemical (weight loss) method in 0.5, 1.0 and 2.0 M HNO<sub>3</sub> solutions and by electrochemical methods such as potentiodynamic polarization (PDP), AC-impedance spectroscopy (AC-IS) and linear polarization resistance in 1.0 M HNO<sub>3</sub> solution at room temperature. Both chemical and electrochemical techniques showed that 8QSC is an efficient green corrosion inhibitor for copper and the efficiency reached 90.4% by weight loss method and 88.4% by AC-IS method at optimum concentration of (300 ppm) 8QSC. The adsorption behavior of 8QSC on copper metal in acid medium obeyed the Langmuir isotherm. The thermodynamic parameters of the adsorption processes were calculated and discussed. AC-IS technique exhibits one capacitive loop, indicating that the corrosion reaction was controlled by charge transfer process. The PDP curves revealed that 8QSC acts as a mixed-type inhibitor. Protective layer of 8QSC on copper surface was examined by SEM, AFM and FT-IR techniques. The experimental results corroborated with results obtained from theoretical DFT studies.

**Keywords** Cu · HNO<sub>3</sub> · 8QSC · AFM · DFT

## Introduction

Copper is a metal that has a wide range of applications due to its excellent electrical conductivity, good mechanical workability, low cost and other relatively noble properties [1, 2]. Therefore, corrosion of copper and its inhibition in a wide variety of media have attracted the attention of many investigators [3–8]. The use of organic inhibitors, especially heterocyclic compounds, is considered as the most effective corrosion inhibitors for the protection of metals and alloys from corrosive media [9–11]. In most acid corrosion, the inhibitors are organic compounds which contain heteroatoms such as nitrogen, sulfur, oxygen, phosphorus and aromatic rings [12–15]. The corrosion inhibition is a surface process, which involves adsorption of the inhibitor molecule on the metal/alloy surface [16]. The adsorbed organic compounds on metal/alloy surface decrease the corrosion rate [17–19]. The adsorption of an inhibitor onto a metal/alloy surface depends on the nature as well as the surface charge of the metal/alloy, the adsorption mode, its chemical structure and the type of the electrolyte solution [1]. The adsorption of inhibition takes place through the heteroatom such as nitrogen, oxygen, sulfur and phosphorus, double bonds or aromatic rings. Generally, the tendency to form a stronger coordination bond results in an increase in inhibition efficiency in the order O < N < S < P [20]. Molecules that at the same time contain nitrogen and sulfur in their structures are of particular importance, since these provide excellent inhibition compared with the compounds that contain only sulfur or nitrogen. Therefore, the selection of an inhibitor is

---

R. Ganapathi Sundaram (✉)  
Department of Chemistry, Faculty of Science and Humanities,  
Mahendra Engineering College (Autonomous), Mallasamudram,  
Namakkal, Tamil Nadu 637 503, India  
e-mail: chemistryganpath17@gmail.com

R. Ganapathi Sundaram · G. Vengatesh · M. Sundaravadivelu  
Department of Chemistry, The Gandhigram Rural Institute-  
Deemed University, Gandhigram, Tamil Nadu 624 302, India

M. Thamaraiselvi  
Department of Chemistry, K. Ramakrishnan College of  
Engineering, Samayapuram, Trichy, Tamil Nadu 621 112, India

very important. In acidic media, heterocyclic organic molecules are easily protonated, and the protonated species may be adsorbed on the metal/alloy surface and protect the metal/alloy from the corrosive environment. The choice of 8-quinoline sulphonyl chloride (8QSC) as corrosion inhibitor is based on the following considerations: this molecule (a) contains one sulfur atom, one nitrogen atom, two oxygen atoms and an aromatic ring as active centers (b) exhibits high solubility in acidic media and (c) it is commercially available, low cost, non-toxic and biodegradable. Quantum chemical calculations have been used recently to explain the corrosion inhibition mechanism [21]. Previously, some work has been done in our laboratory on mild steel in 1.0 M HCl and in 1.0 M H<sub>2</sub>SO<sub>4</sub> with the same inhibitor, i.e., 8QSC [12, 22]. The percentage inhibition of 8QSC on mild steel in 1.0 M HCl was 81.6% and in 1.0 M H<sub>2</sub>SO<sub>4</sub> was 87.1% at room temperature.

The aim of the present manuscript is to evaluate the inhibition effect of 8QSC on the corrosion of copper in 0.5, 1.0 and 2.0 M HNO<sub>3</sub> solutions. The study was conducted by using weight loss measurements, electrochemical measurements and surface investigation techniques namely scanning electron microscope (SEM), atomic force microscope (AFM) and Fourier transform-infrared spectroscopy (FT-IR). The earlier result of quantum chemical calculations was correlated with the experimental results.

## Materials and Experimental Techniques

### Preparation of Copper Metal Specimen

The corrosion inhibition study was performed on 99.9% purity of copper metal specimen. The copper metal specimens with area of 3.5 × 1.5 × 0.2 cm<sup>3</sup> were used for weight loss measurements. Copper metal strips with area of 1.0 × 1.0 × 0.2 cm<sup>3</sup> were used for surface morphological study. For the electrochemical investigation, a copper rod set in commercially available epoxy resin having a 1.0 cm<sup>2</sup> circular cross-sectional area was exposed to 100 mL of aerated 1.0 M nitric acid (HNO<sub>3</sub>) solution. The surfaces of all the specimens were mechanically abraded with different grades of emery papers (1/0 to 7/0), washed with double distilled water and then degreased with acetone. Finally, they were dried in air before use.

### Preparation of Corrosive Solution

The analytical grade 69.0% nitric acid was purchased from Merck India, and the corrosive solutions of 0.5 M HNO<sub>3</sub>, 1.0 M HNO<sub>3</sub> and 2.0 M HNO<sub>3</sub> were prepared by dilution of nitric acid with double distilled water.

### Preparation of Inhibitor Solution

The investigated quinoline nucleus-based drug molecule 8QSC was purchased from *Sigma-Aldrich* and used as a green corrosion inhibitor in HNO<sub>3</sub> solution on copper metal surfaces. The molecular structure and optimized structure of 8-quinoline sulphonyl chloride are given in Fig. 1a and b. The preparation of various concentrations of inhibitor solution was done according to the standard method as described earlier [23].

### Weight Loss Experiment

In weight loss experiments, the pre-cleaned and pre-weighed seven copper specimens were immersed in 100 mL of 0.5, 1.0 and 2.0 M aerated corrosive solution with and without addition of different concentrations of 8QSC for a period of 3 h. After that, the copper specimens were taken out from the aerated test solutions, washed with double distilled water, dried with an air drier and finally weighed. The corrosion rate (CR), and the percentage of inhibition efficiency (IE%) were calculated by the following equations:

$$CR = W = \frac{m_1 - m_2}{St} \quad (\text{Eq 1})$$

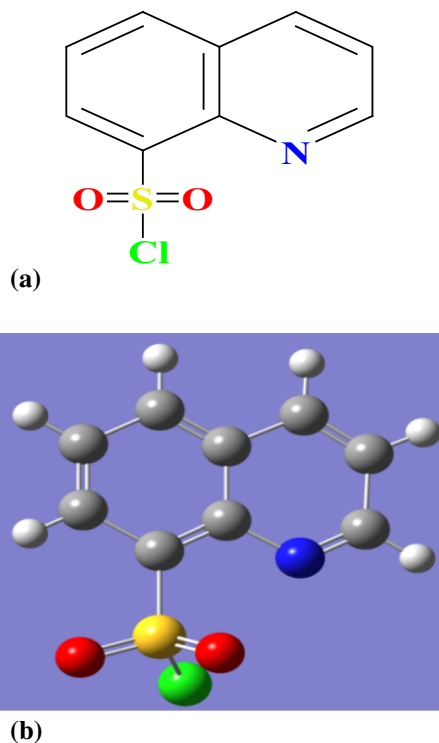


**Fig. 1** (a) Molecular structure of 8QSC and (b) optimized structure of 8QSC

$$IE (\%) = \left[ \frac{W_o - W_i}{W_o} \right] \times 100 \quad (\text{Eq 2})$$

where  $W$  is rate, loss per unit time and area of copper specimen,  $m_1$  and  $m_2$  are the weight of the specimen before and after corrosion,  $S$  is the total surface area of the specimen,  $t$  is the immersion time of the specimen,  $W_o$  and  $W_i$  are the corrosion rates in the absence and presence of 8QSC, respectively.

### Electrochemical Experiments

Electrochemical experiments were conducted using CH-Electrochemical analyzer model 760 D with CHI 760 D software. A three-electrode electrochemical cell system consists of the copper as working electrode, saturated calomel electrode (SCE) as a reference electrode and a platinum wire as an auxiliary or counter electrode. Before starting the electrochemical experiment, the working electrode was immersed in the corrosive solution for 30 min at room temperature until a steady-state open circuit potential ( $E_{\text{OCP}}$ ) was obtained. The AC-impedance spectroscopy (AC-IS) experiments were taken at the OCP in the frequency range from 10 kHz to 0.1 Hz with AC-impedance signal of 0.01 V amplitude. From this experiment, the impedance plots like Nyquist and Bode were generated. The charge transfer resistance ( $R_{\text{ct}}$ ) and double-layer capacitance ( $C_{\text{dl}}$ ) values were obtained from the Nyquist plots, and the inhibition efficiency (IE) was calculated from the following equation:

$$IE (\%) = \left[ \frac{R_{\text{ct}}^i - R_{\text{ct}}^o}{R_{\text{ct}}^i} \right] \times 100 \quad (\text{Eq 3})$$

where  $R_{\text{ct}}^i$  and  $R_{\text{ct}}^o$  are the charge transfer resistance values measured in the presence and absence of 8QSC in 1.0 M  $\text{HNO}_3$ , respectively.

Potentiodynamic polarization (PDP) experiments were performed using the same three cell system that was used in AC-IS experiments. The PDP curves were recorded by changing the electrode potential automatically from  $-300$  to  $+300$  mV with respect to OCP at a constant sweep rate 0.1 mV/s and under air atmosphere. From this experiment, the inhibition efficiency was calculated from corrosion current density ( $I_{\text{corr}}$ ) values by the formula:

$$IE (\%) = \left[ \frac{I_{\text{corr}}^o - I_{\text{corr}}^i}{I_{\text{corr}}^o} \right] \times 100 \quad (\text{Eq 4})$$

where  $I_{\text{corr}}^o$  and  $I_{\text{corr}}^i$  are the corrosion current density values measured in the absence and presence of 8QSC in 1.0 M  $\text{HNO}_3$ , respectively.

Linear polarization resistance measurements (LPR) were carried out by the potential of the electrode scanned

from  $-0.02$  to  $+0.02$  V versus  $E_{\text{corr}}$  at a scan rate of 0.125 mV/s. The inhibition efficiency (IE%) was calculated using the following relationship [22].

$$IE (\%) = \left[ \frac{R_p^i - R_p^o}{R_p^i} \right] \times 100 \quad (\text{Eq 5})$$

where  $R_p^i$  and  $R_p^o$  are the linear polarization resistance values measured in the presence and absence of 8QSC molecule in 1.0 M  $\text{HNO}_3$ , respectively.

### Surface Morphology Investigations

#### SEM Studies

For surface morphological study, the surface features of fresh, abraded and cleaned copper specimen and copper specimens were immersed in 1.0 M  $\text{HNO}_3$  solution in the absence and presence of optimum concentration (300 ppm) of 8QSC for 3 h at room temperature were analyzed by using a JEOL/EO JSM—6390 model SEM.

#### AFM Studies

For surface topographical study, the surface features of fresh, abraded and cleaned copper were examined before and after exposure to 1.0 M  $\text{HNO}_3$  solutions for 3 h without and with the optimum concentration of 8QSC. The “NT-MDT multimode modular AFM” instrument was used for this investigation. The scanning area of all the AFM images was  $4 \mu\text{m} \times 4 \mu\text{m}$  and the scan rate was 1.0 Hz per line.

#### FT-IR Studies

The FT-IR spectra were also recorded with a frequency ranging from 4000 to  $400 \text{ cm}^{-1}$  with a resolution of  $4 \text{ cm}^{-1}$  for the pure 8QSC as well as the 8QSC adsorbed on copper metal in 1.0 M  $\text{HNO}_3$  solution in KBr matrix using JASCO 460 PLUS spectrophotometer.

### Theoretical Studies: Quantum Chemical Calculations

Quantum chemical calculations of the investigated inhibitor molecule 8QSC were performed by using density functional theory (DFT) method [24], and the geometry of the studied inhibitor molecule 8QSC was optimized using DFT/B3LYP having the basis set 6-31+G (d, p) [25]. DFT/B3LYP is recommended for the study of chemical reactivity and selectivity in terms of frontier molecular orbital theory [10].

## Results and Discussion

### Weight Loss (WL) Experiments

A major advantage of weight loss experiments is its relative simplicity and availability [26]. The results obtained for the surface protection of copper in 0.5, 1.0 and 2.0 M HNO<sub>3</sub> solutions containing different concentrations (50–300 ppm) of 8QSC from weight loss experiments are given in Fig. 2 as well as Table 1. The corrosion parameters like corrosion rate and percentage of inhibition efficiency were determined for 3-h immersion period by using Eqs 1 and 2. The results indicate that the IE% increases with increasing concentration of 8QSC in 0.5 and 1.0 M HNO<sub>3</sub> solution but IE% was decreased in 2.0 M HNO<sub>3</sub> solution. Because the inhibitor molecules adsorbed on the corroded copper metal surface in 0.5 and 1.0 M HNO<sub>3</sub> medium but in higher molar concentration (2.0 M HNO<sub>3</sub>) of corrosive medium desorption may take place. That is the rate of chemical reaction was increased and also controls the adsorption behavior of inhibitor molecule by the ionization of active species associated with the inhibitor molecule [27]. From this weight loss experiments, the maximum IE% was obtained in 1.0 M HNO<sub>3</sub> solution at optimum concentration (300 ppm) of 8QSC (Table 2); hence, further studies such as electrochemical corrosion testing and surface morphology were also conducted in 1.0 M HNO<sub>3</sub> solution.

### Adsorption Isotherm Studies

Adsorption isotherms are used to understand the mode of interactions between inhibitor molecules and the metal/

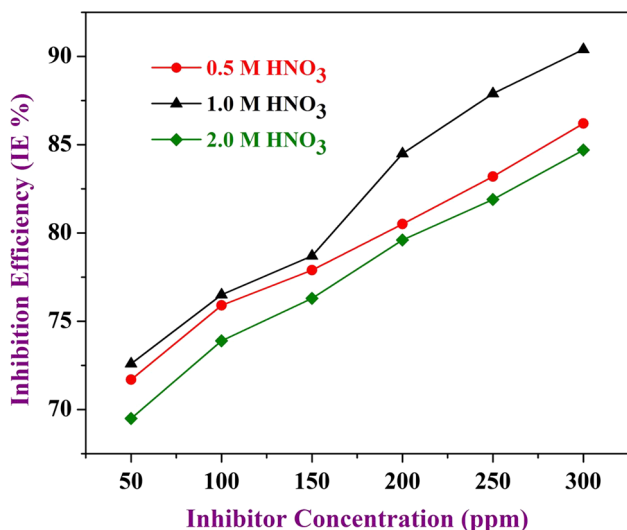


**Fig. 2** Plot of inhibition efficiency for Cu metal in 0.5, 1.0 and 2.0 molar solution of HNO<sub>3</sub> in the presence of various concentrations of 8QSC by weight loss experiment

alloy surface. The adsorption of the inhibitor molecules on metal/alloy surfaces never reaches the real equilibrium but tends to reach an adsorption steady state [28]. When the corrosion rate is decreased in the presence of optimum concentration of inhibitor, the adsorption process has a tendency of attaining a state of quasi-equilibrium [29, 30]. The nature of quasi-equilibrium adsorption of inhibitors can be investigated using the appropriate adsorption isotherm. The most frequently used adsorption isotherms are Temkin, Freundlich and Langmuir isotherms. Attempts to fit data obtained from the WL, AC-IS, PDP and LPR studies into different adsorption isotherms (Temkin, Freundlich and Langmuir) revealed that the data best fit to the Langmuir adsorption isotherm. According to Langmuir adsorption isotherm,  $\theta$  is related to  $C_{inh}$  by the following equation:

$$\frac{C_{inh}}{\theta} = \frac{1}{K_{ads}} + C_{inh} \tag{Eq 6}$$

where  $C_{inh}$  is the 8QSC concentration (ppm),  $\theta$  is the degree of surface coverage and  $K_{ads}$  is the equilibrium constant of the adsorption process.

**Table 1** The effect of different molar solution of HNO<sub>3</sub> on copper corrosion with various concentrations of 8QSC after immersion of 3 h at room temperature

Conc. of 8QSC (ppm)	Different molar solution of Nitric acid					
	0.5 M Nitric acid		1.0 M Nitric acid		2.0 M Nitric acid	
	CR	IE (%)	CR	IE (%)	CR	IE (%)
Nitric acid	29.88	...	32.73	...	32.18	...
50	8.45	71.7	8.97	72.6	9.82	69.5
100	7.21	75.9	7.70	76.5	8.41	73.9
150	6.59	77.9	6.97	78.7	7.62	76.3
200	5.82	80.5	5.07	84.5	6.55	79.6
250	5.03	83.2	3.93	87.9	5.80	81.9
300	4.11	86.2	3.13	90.4	4.92	84.7

**Table 2** The effect of various concentrations of 8QSC on copper surface in 1.0 M HNO<sub>3</sub> solution after immersion of 3 h at room temperature

Conc. of 8QSC (ppm)	Weight loss (mg/cm <sup>2</sup> )	Corrosion rate (mm/y)	IE (%)
1.0 M nitric acid	9.82	32.73	...
50	2.69	8.97	72.6
100	2.31	7.70	76.5
150	2.09	6.97	78.7
200	1.52	5.07	84.5
250	1.18	3.93	87.9
300	0.94	3.13	90.4

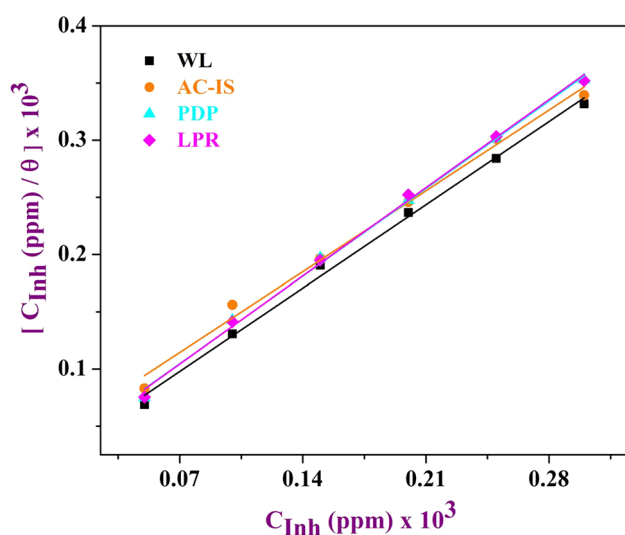


**Fig. 3** Langmuir plot (using WL, AC-IS, PDP and LPR results) for corrosion of copper metal in 1.0 M HNO<sub>3</sub> solution with various concentrations of 8QSC

The correlation between  $K_{\text{ads}}$  and  $\Delta G_{\text{ads}}^0$  (standard free energy of adsorption) is given by equation:

$$\Delta G_{\text{ads}}^0 = -RT \ln ( 55.5 K_{\text{ads}} ) \quad (\text{Eq 7})$$

where  $R$  is the universal gas constant,  $T$  is the absolute temperature and 55.5 is the concentration of water in solution in mol/L. The Langmuir adsorption isotherm was drawn by plotting  $C_{\text{inh}}/\theta$  versus  $C_{\text{inh}}$  for various concentrations of 8QSC and considering the  $\theta$  values from the WL method at 3 h, AC-IS, PDP and LPR studies at room temperature for copper in 1.0 M HNO<sub>3</sub>, and the plots are shown in Fig. 3. The calculated values of  $\Delta G_{\text{ads}}^0$ ,  $K_{\text{ads}}$  and  $R^2$  are given in Table 3. The slope of the  $C_{\text{inh}}/\theta$  versus  $C_{\text{inh}}$  plot shows that the  $R^2$  values are nearly equal to one (WL 0.9957, AC-IS 0.9924, PDP 0.9976 and LPR 0.9977) which implies that it obeys the Langmuir adsorption isotherm [31]. Generally, the value of  $\Delta G_{\text{ads}}^0$  around  $-20$  kJ/mol or less negative implies that the adsorption is due to electrostatic interaction, i.e., physisorption, while a value of  $\Delta G_{\text{ads}}^0$  around  $-40$  kJ/mol or more negative suggests that the adsorption is chemisorption. In the present study, the  $\Delta G_{\text{ads}}^0$  values obtained from all methods (WL, AC-IS, PDP and LPR) are less than  $-20$  kJ/mol, which suggests that the adsorption of the investigated inhibitor on copper metal surface is strongly physisorption and the process is always spontaneous.

## Electrochemical Experiments

### AC-Impedance Spectroscopy (AC-IS) Measurements

Table 4 shows the results obtained from AC-IS measurements for the corrosion of copper in the absence and the

**Table 3** Thermodynamic parameters for the adsorption of 8QSC on copper surface in 1.0 M HNO<sub>3</sub> solution

Method	$R^2$	$K_{\text{ads}}$ ( $10^4 \text{ M}^{-1}$ )	$\Delta G_{\text{ads}}^0$ (kJ/mol)
WL	0.9957	41.6351	− 19.51
AC-IS	0.9924	23.0530	− 18.02
PDP	0.9976	39.1154	− 19.35
LPR	0.9977	40.3815	− 19.43

**Table 4** AC-impedance spectroscopy parameters obtained from electrochemical studies of copper in 1.0 M HNO<sub>3</sub> solution with various concentrations of 8QSC

Conc. of 8QSC (ppm)	$Y_{\text{max}}$ ( $\Omega\text{cm}^2$ )	$R_{\text{ct}}$ ( $\Omega\text{cm}^2$ )	$C_{\text{dl}}$ ( $\mu\text{F}/\text{cm}^2$ )	IE (%)
1.0 M nitric acid	4.151	8.354	4591.9	...
50	10.442	21.039	724.82	60.3
100	11.506	23.225	595.88	64.0
150	17.382	35.153	260.60	76.2
200	22.169	44.643	160.89	81.3
250	24.521	49.026	132.45	83.0
300	35.848	71.948	61.738	88.4

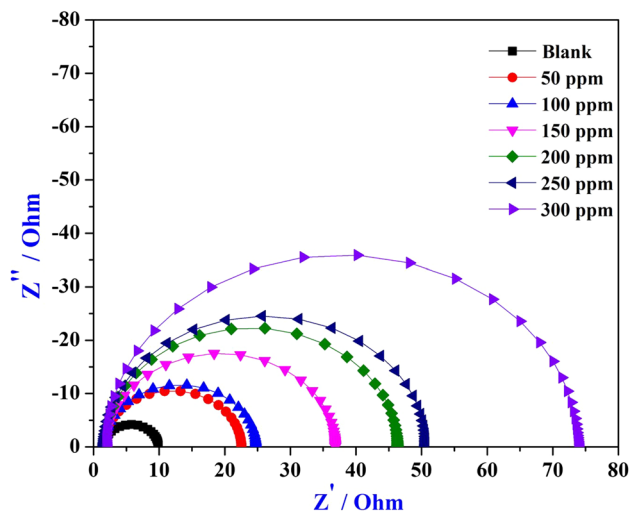


**Fig. 4** Nyquist plot for copper corrosion in 1.0 M HNO<sub>3</sub> in the absence and presence of various concentrations of 8QSC

presence of various concentrations of 8QSC at room temperature. The impedance spectra obtained for copper in 1.0 M HNO<sub>3</sub> solution in the absence and presence of various concentrations of tested inhibitor at room temperature are presented as Nyquist plots in Fig. 4. Figure 4 suggests that the impedance spectra exhibit a depressed capacitive loop, which has the center below the real axis, indicating the roughness and the inhomogeneities at the copper electrode [32].

The diameter of the capacitive loops in the presence of 8QSC is bigger than the absence of 8QSC and also the diameter of the loop increases with the increase in inhibitor concentration [33, 34]. This indicates that the impedance of inhibited substrate increases with the inhibitor concentration. Noticeably, these capacitive loops are not perfect semicircles, which can be attributed to the frequency dispersion effect. This anomalous behavior is generally attributed to the roughness and in-homogeneity of the copper electrode [35]. The simplest fitting is represented by Randles electrical equivalent circuit in Fig. 5, which is a parallel combination of the charge transfer resistance,  $R_{ct}$  and the constant phase element,  $CPE_{dl}$  both in series with the solution resistance ( $R_s$ ) [36]. It is seen that, the addition of inhibitor increases the values of charge transfer resistance ( $R_{ct}$ ) and reduces the double-layer capacitance ( $C_{dl}$ ). The interfacial double-layer capacitance ( $C_{dl}$ ) values have been calculated from the impedance value using Nyquist plot by the following formula:

$$C_{dl} = (2\pi f_{max} R_{ct})^{-1} \tag{Eq 8}$$

The values of  $C_{dl}$  decreased with an increase in the inhibitor concentration. This is due to an increase in the surface coverage by 8QSC, resulting in an increase in the inhibition efficiency (IE%). The thickness of the protective layer  $\delta_{inh}$  was related to  $C_{dl}$  by the equation [37]:

$$\delta_{inh} = \frac{\epsilon_0 \epsilon_r}{C_{dl}} \tag{Eq 9}$$

where  $\epsilon_0$  is the dielectric constant and  $\epsilon_r$  is the relative dielectric constant. Decrease in the capacitance leading to decrease in the local dielectric constant or increase in the thickness of the electrical double-layer strongly suggests that the 8QSC molecules are adsorbed at the copper/1.0 M HNO<sub>3</sub> solution interface [38]. The increase in  $R_{ct}$  values on the addition of 8QSC indicates the formation of protective film at the copper/nitric acid solution interface. These observations suggest that the tested inhibitor 8QSC molecules adsorbed on the copper surface.  $R_{ct}$  values were used to determine the IE%, according to Eq 3. Figure 6 shows both the Bode-modulus and phase angle plots recorded for the copper electrode immersed in 1.0 M HNO<sub>3</sub> solution in

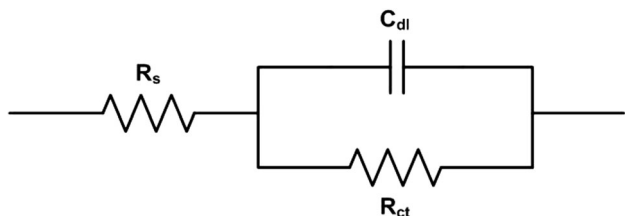


**Fig. 5** Electrical equivalent circuit used for fitting and analyzing the electrochemical data ( $R_s$  solution resistance,  $R_{ct}$  charge transfer resistance,  $C_{dl}$  double-layer capacitance)

the absence and presence of various concentration of 8QSC.

The phase angle at high frequencies provides a general idea of the anticorrosion activity of 8QSC molecules. The more negative of the phase angle, the more capacitive of the electrochemical behavior [12]. From Fig. 6, the phase angle increases with increase in the studied 8QSC molecule concentration; this is due to the adsorption of the inhibitor molecule on the copper surface [39]. According to the appearance of the phase angles versus frequency diagrams, the increasing concentration of the studied green corrosion inhibitor 8QSC in the presence of nitric acid solution results in more negative values of the phase angle at high frequencies, indicating superior inhibitive behavior at higher concentrations. This result could be attributed to higher corrosion activity even at low concentrations of 8QSC [40, 41].

*Potentiodynamic Polarization (PDP) Measurements*

The kinetics of the anodic and cathodic reactions occurring on a copper electrode in free acid (1.0 M HNO<sub>3</sub>) solution and various concentrations of 8QSC in 1.0 M HNO<sub>3</sub> solution were investigated through the potentiodynamic polarization measurements. The IE% was calculated according to Eq 4, and the obtained results are given in Table 5. Table 5 shows that copper specimen in 1.0 M HNO<sub>3</sub> solution with 8QSC has a lower  $I_{corr}$  value than that of the copper specimen in the free acid solution. This reveals that the inhibitor molecule decreases the corrosion current ( $I_{corr}$ ) and thus reduces the corrosion rate (CR). In 1.0 M HNO<sub>3</sub> solution with 50 ppm of 8QSC, the  $I_{corr}$  value was 0.1153 and the IE% was 66.5. After the addition of optimum concentration (300 ppm) of 8QSC, the  $I_{corr}$  value

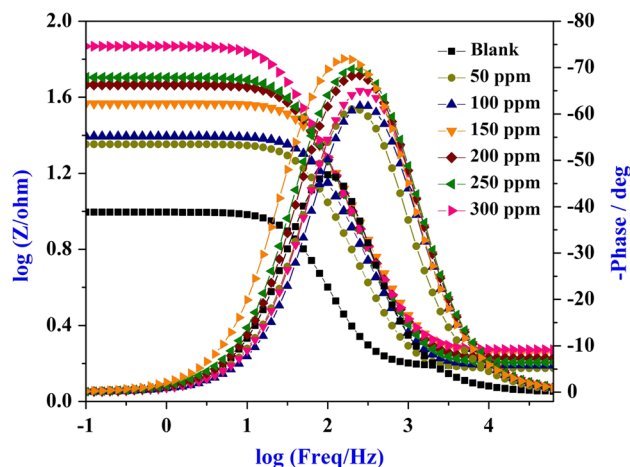


**Fig. 6** Bode-modulus and phase angle plots for copper corrosion in 1.0 M HNO<sub>3</sub> in the absence and presence of various concentrations of 8QSC

was reduced from 0.1153 to 0.0518 and IE% was increased from 66.5 to 85.0. A lower  $I_{\text{corr}}$  value for 8QSC in 1.0 M  $\text{HNO}_3$  solutions implies that the rate of electrochemical reactions was reduced owing to the formation of a barrier film over the electrode (copper) surface by the studied inhibitor molecules [42]. That is,  $I_{\text{corr}}$  value is indirectly proportional to IE%. This study clearly shows that the investigated inhibitor molecules 8QSC are adsorbed on the copper electrode surface and also blocked the active sites of the copper metal in 1.0 M  $\text{HNO}_3$  solution [43]. Figure 7 shows the polarization curves for copper at various concentrations of 8QSC in 1.0 M  $\text{HNO}_3$  solution. It is observed that both the cathodic and anodic reactions are suppressed with the addition of 8QSC, which suggests that it inhibits both anodic dissolution and cathodic hydrogen evolution reactions [32].

These experimental results indicate that the addition of 8QSC may affect the anodic and the cathodic corrosion

**Table 5** Polarization parameters obtained from electrochemical studies of copper in 1.0 M  $\text{HNO}_3$  solution with various concentrations of 8QSC

Conc. of 8QSC (ppm)	$\beta_a$ (V/dec)	$\beta_c$ (V/dec)	$E_{\text{corr}}$ (mV/SCE)	$I_{\text{corr}}$ (mA/cm <sup>2</sup> )	IE (%)
1.0 M nitric acid	10.887	3.465	19	0.3442	...
50	14.746	2.698	14	0.1153	66.5
100	14.697	3.343	15	0.1046	70.0
150	15.230	3.357	17	0.0823	76.1
200	15.613	3.752	16	0.0662	80.8
250	15.258	3.124	16	0.0596	83.0
300	15.899	3.680	21	0.0518	85.0

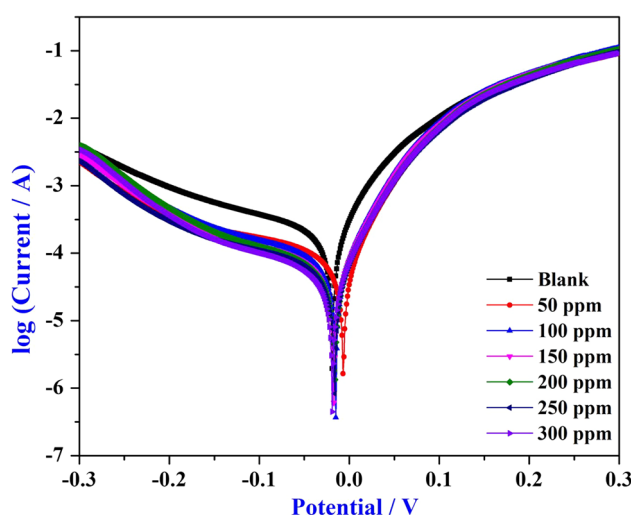


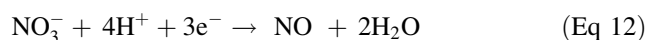
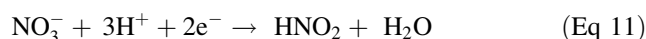
**Fig. 7** Potentiodynamic polarization curves for copper corrosion in 1.0 M  $\text{HNO}_3$  in the absence and presence of various concentrations of 8QSC

reaction. According to Ferreira and others [44, 45], if the displacement of corrosion potential ( $E_{\text{corr}}$ ) is greater than 85 mV with respect to the corrosion potential of the blank solution, the inhibitor can be seen as a cathodic or anodic type. In the present study, there was no significant change in the  $E_{\text{corr}}$  values in the presence of 8QSC, which suggests that 8QSC is a mixed-type inhibitor [46, 47]. The electrochemical anodic and cathodic reactions of copper in aerated 1.0 M  $\text{HNO}_3$  solution can be described as follows [48]:

Anodic reaction:



Cathodic reactions:



#### Linear Polarization Resistance (LPR) Measurements

The linear polarization resistance parameters were obtained from the slope of the potentiodynamic polarization curves. The IE% was calculated by using above-mentioned Eq 5, and the values are given in Table 6. The results showed that the  $R_p$  values increased with increase in the concentration of evaluated inhibitor. The increase in the inhibition efficiencies for corrosion of copper metal in 1.0 M  $\text{HNO}_3$  solution with increasing concentration of 8QSC can be explained on the basis of adsorption [16]. This study clearly confirmed the formation of a surface film on the working electrode.

#### Surface Morphological Investigation

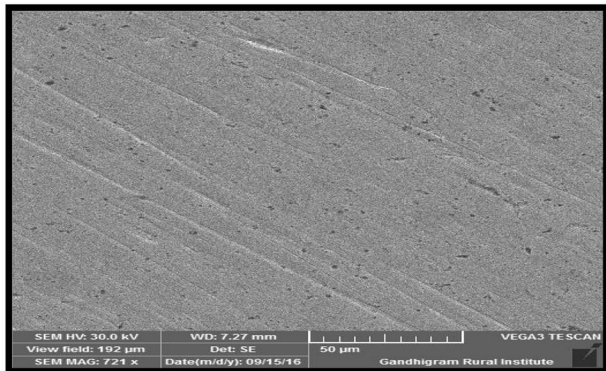
##### SEM Analysis

The surface morphologies of fresh-abraded copper metal, copper metal in free acid (blank) solution and copper metal

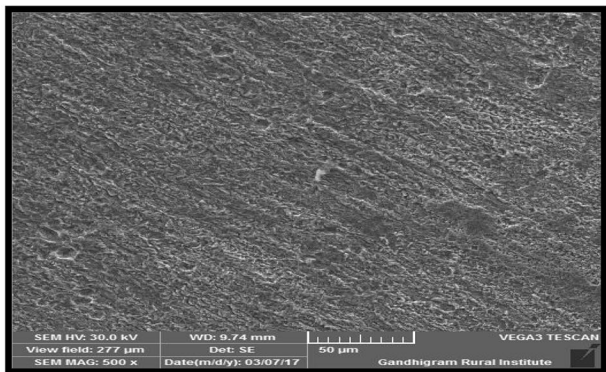
**Table 6** LPR parameters obtained from electrochemical studies of copper metal in 1.0 M  $\text{HNO}_3$  solution with various concentrations of 8QSC

Conc. of 8QSC (ppm)	$R_p$ ( $\Omega\text{cm}^2$ )	IE (%)
1.0 M nitric acid	68	...
50	202	66.3
100	232	70.7
150	294	76.9
200	328	79.3
250	386	82.4
300	458	85.2

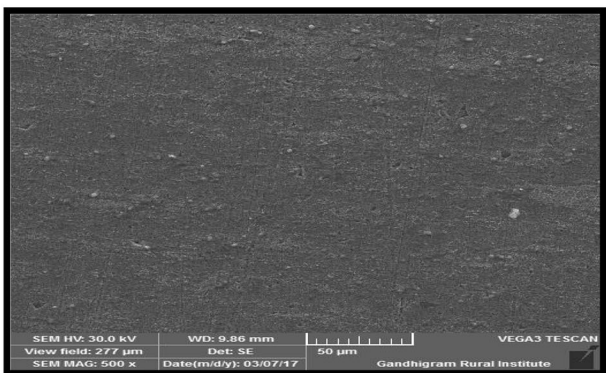
in 1.0 M HNO<sub>3</sub> solution with optimum concentration of 8QSC are shown in Fig. 8a, b and c, respectively. The SEM image of copper metal surface exposed to the inhibitor-acid solution (8c) shows less surface damage than the surface exposed only to free acid (1.0 M HNO<sub>3</sub>) solution (8b) which reveals a generalized corrosion effect. The increased surface smoothness in the presence of 8QSC is attributed due to the adsorption of 8QSC on the copper metal surface [49]. From this investigation, we confirmed that the inhibitor-treated copper metal surfaces are smooth and protected from acid attack.



(a)



(b)



(c)

**Fig. 8** SEM images of copper surfaces: (a) fresh-abraded Cu (b) Cu in free acid solution and (c) Cu in inhibitor-acid solution

*AFM Analysis*

Atomic Force Microscopy (AFM) analysis was also carried out to evaluate the average surface roughness of fresh-abraded copper metal, copper metal in free acid solution and copper metal in inhibitor-acid solution. The two-dimensional (2D) and three-dimensional (3D) photographs of fresh-abraded copper metal, copper metal in free acid solution and copper metal in inhibitor-acid solution are shown in Figs. 9a, b, 10a, b, and 11a, b. Some important AFM parameters of the above copper metals are summarized in Table 7.

In free acid solution (Fig. 10b), the copper metal surface indicates a mountain like photographs due to unhindered corrosion attack and the average surface roughness is 79.14 nm. In an inhibitor-acid solution, the copper metal implies a smoother surface (Fig. 11b) and the average surface roughness value is 16.06 nm, which suggest that the formation of a protective film (mono layer) of 8QSC on the corroded copper metal surface.

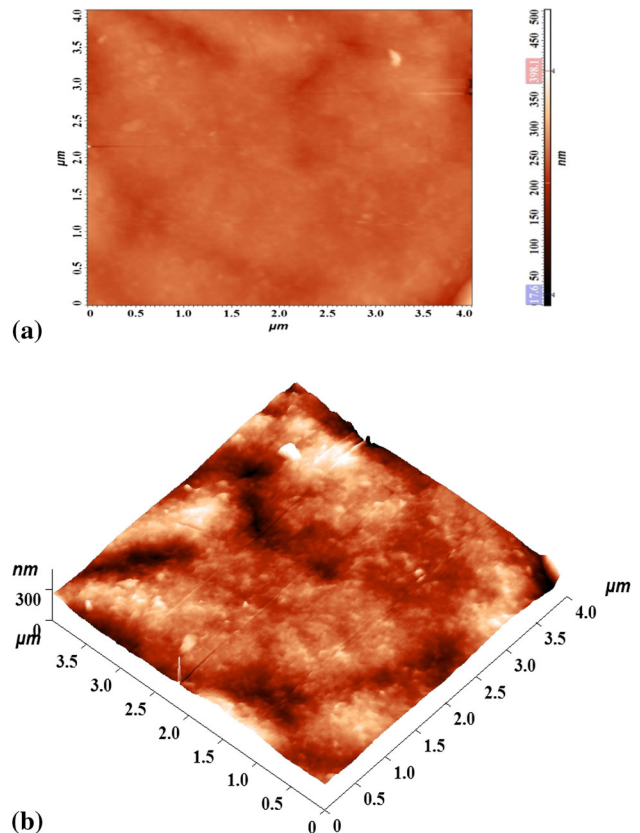


**Fig. 9** Topography AFM images of fresh-abraded Cu: (a) two-dimensional structure and (b) three-dimensional structure



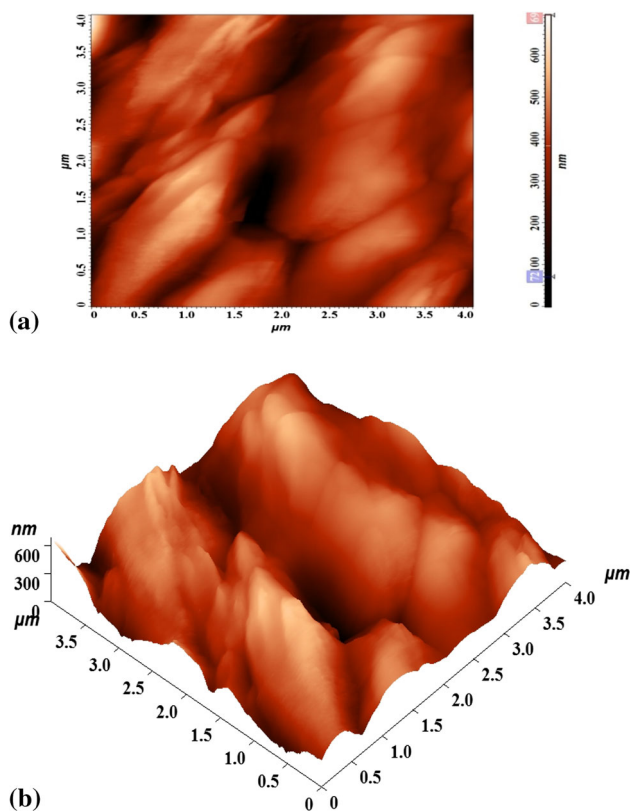


**Fig. 10** Topography AFM images of Cu in free acid solution: (a) two-dimensional structure and (b) three-dimensional structure

#### FT-IR Analysis

FT-IR spectra were recorded for the characterization of the pure 8QSC and scratched protective film formed 8QSC over the copper metal surface and are given in Fig. 12. The frequencies are shown in Table 8. The pure 8QSC shows a broad band at  $3082\text{--}3009\text{ cm}^{-1}$  is attributed to aromatic C–H stretching. The band at  $1542\text{--}1588\text{ cm}^{-1}$  is assigned to aromatic C=C stretching vibrations [50, 51]. The absorption band at  $1624\text{ cm}^{-1}$  corresponds to the C=N stretching vibration. The band at  $1247\text{--}1189\text{ cm}^{-1}$  indicates the stretching vibration of  $\text{SO}_2$ . Hence, it can be inferred that pure 8QSC contains oxygen, nitrogen and sulfur atoms in functional groups and C=C in an aromatic ring, which meets the general structural consideration of this class of corrosion inhibitors [52]. The FT-IR spectrum of scratched material shows that the band at  $3082\text{--}3009\text{ cm}^{-1}$  is shifted to  $3060\text{--}2920\text{ cm}^{-1}$ . The C=N stretching frequency has shifted from  $1624$  to  $1632\text{ cm}^{-1}$ , indicating the quinoline ring nitrogen is protonated. The  $\text{SO}_2$  group is shifted downwards from  $1189$  to  $1153\text{ cm}^{-1}$ . Moreover, the bands at  $1542\text{--}1588\text{ cm}^{-1}$  in scrapped material are not present, which indicates the interaction of C=C in the aromatic ring

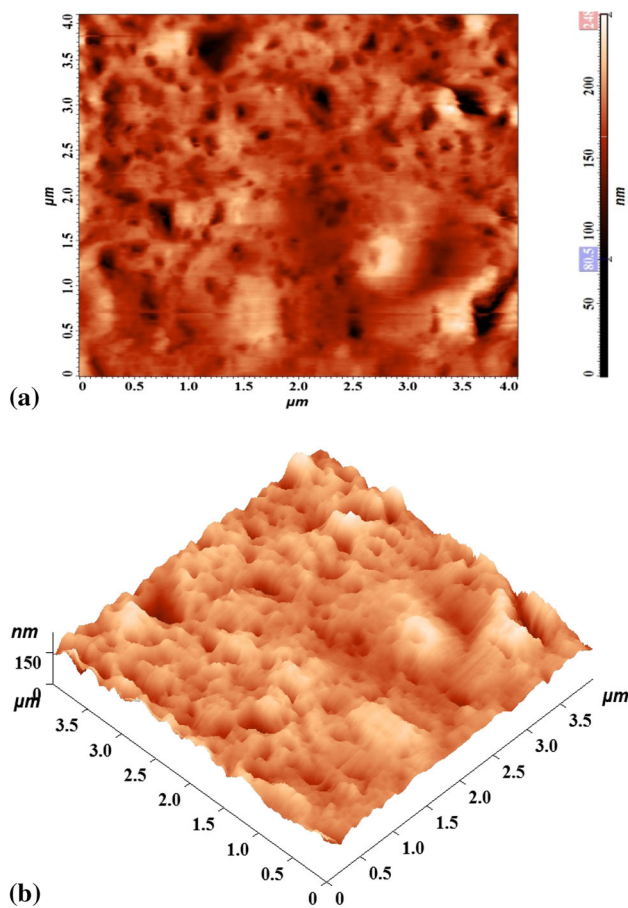


**Fig. 11** Topography AFM images of Cu in inhibitor-acid solution: (a) two-dimensional structure and (b) three-dimensional structure

**Table 7** AFM parameters obtained data for fresh polished and cleaned Cu metal, Cu metal in the absence and the presence of 8QSC in 1.0 M  $\text{HNO}_3$

Sample	Root mean square roughness (nm)	Maximum peak-to-peak height (nm)	Ten-point height (nm)	Average roughness (nm)
Fresh, polished and cleaned Cu	12.01	501.36	236.47	8.87
Cu in 1.0 M nitric acid solution	97.63	695.77	348.34	79.14
Cu in 8QSC-nitric acid solution	21.71	248.72	125.41	16.06

with the copper metal surface. The comparing of the two spectra clearly indicates the interaction of the lone pair of electrons in the heteroatoms and  $\pi$  electrons of C=C with

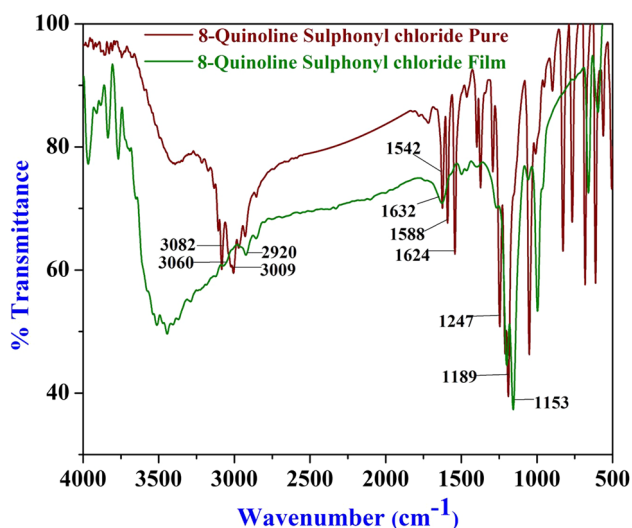


**Fig. 12** FT-IR spectra of inhibitor (Pure) and its corresponding film formed copper surface after immersion in 1.0 M HNO<sub>3</sub> solution containing 300 ppm of 8QSC at room temperature

**Table 8** FT-IR spectrum frequency for pure 8QSC and protective film formation of 8QSC on copper metal

Group responsible	IR frequency of pure 8QSC (cm <sup>-1</sup> )	IR frequency of protective film of 8QSC on Cu (cm <sup>-1</sup> )
Aromatic C-H	3082–3009	3060–2920
Aromatic C=C	1542–1588	...
C=N	1624	1632
SO <sub>2</sub>	1247–1189	1153

the copper metal, leading to the formation of a protective film of 8QSC on the copper metal surface.

#### Theoretical Studies: Quantum Chemical Calculations

Quantum chemical methods were utilized to better understand the relationship between the electronic properties of the molecular structure and the corresponding inhibitive effect on the metal/alloy surface. Furthermore, the results of quantum chemical methods could be obtained without laboratory measurements thus saving time, chemicals and equipment [53]. Due to its accuracy and smaller time requirement for the computational methods, it is widely used to analyze inhibitor efficiencies and inhibitor–surface interactions [54]. Hence, the DFT method with 6-31G (d, p) set 6-31+G (d, p) basis sets of software was used to give some insight into the inhibitive mechanism of 8QSC molecule on the copper metal surface. From this method, the obtained quantum chemical parameters such as highest occupied molecular orbital ( $E_{\text{HOMO}}$ ), lowest unoccupied

molecular orbital ( $E_{\text{LUMO}}$ ), energy gap ( $\Delta E$ ), global electronegativity ( $\chi$ ), absolute hardness ( $\eta$ ) and softness ( $\sigma$ ) are summarized in Table 9.

The HOMO and LUMO electron density distributions of the evaluated inhibitor 8QSC are shown in Fig. 13a and b. The energy of HOMO ( $E_{\text{HOMO}}$ ) is directly related to the ionization potential ( $I$ ), while the energy of LUMO ( $E_{\text{LUMO}}$ ) is directly related to electron affinity ( $A$ ). The  $I$  and  $A$  were calculated according to Koopmans theorem [24]. This theorem drives the relationship between the energies of HOMO and LUMO.  $I$  and  $A$  are related to  $E_{\text{HOMO}}$  and  $E_{\text{LUMO}}$  as follows [55].

$$I = -E_{\text{HOMO}} \quad (\text{Eq 14})$$

$$A = -E_{\text{LUMO}}. \quad (\text{Eq 15})$$

The global electronegativity ( $\chi$ ), absolute hardness ( $\eta$ ) and an absolute softness ( $\sigma$ ) of 8QSC are calculated by the following equations:

$$\chi = (I + A)/2 \quad (\text{Eq 16})$$

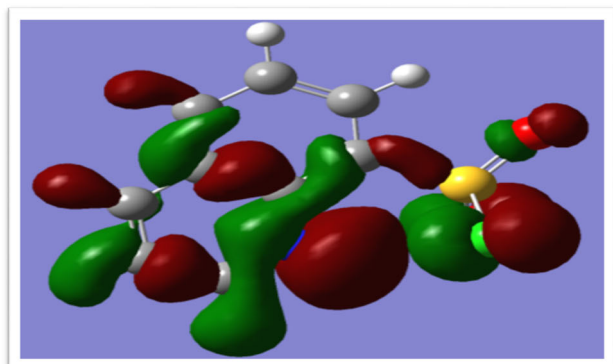
$$\eta = (I - A)/2 \quad (\text{Eq 17})$$

$$\sigma = 1/\eta \quad (\text{Eq 18})$$

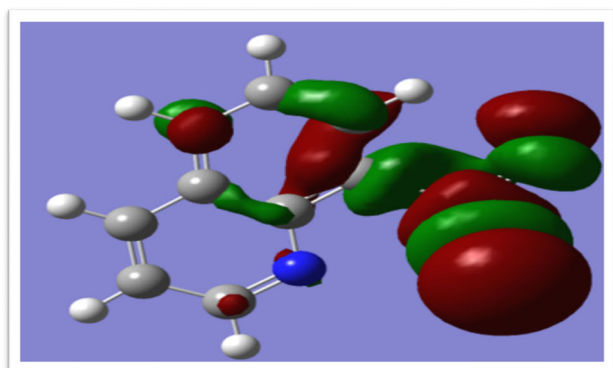
The adsorption of the inhibitor on the metal/alloy surface can occur on the basis of donor–acceptor interactions between the  $\pi$  electrons of the heterocyclic compounds and vacant orbitals of the metal/alloy atoms of the surface [56]. The electron donating ability of the molecule (8QSC) is associated with the  $E_{\text{HOMO}}$ . High values of  $E_{\text{HOMO}}$  reflect the tendency of the inhibitor molecule (8QSC) to donate electrons to the acceptor molecules with low energy empty molecular orbitals. Thus, high values of  $E_{\text{HOMO}}$  stimulate the adsorption process, and hence the inhibition efficiency is enhanced. The ability of a molecule to accept the electrons is related to  $E_{\text{LUMO}}$ . A lower value of  $E_{\text{LUMO}}$  denotes the easier acceptance of electrons from the metal/alloy surface and leads to better inhibition process [57]. The energy gap ( $\Delta E$ ) between the HOMO and LUMO of the inhibitor molecule is also another important factor to determine the inhibition efficiency. Molecules with lower  $\Delta E$  values give higher inhibition efficiency [58]. The  $\Delta E$  value of 8QSC is 0.1074 eV. The dipole moment ( $\mu$ ) is another way to obtain data on the electronic distribution in a molecule and is one of the properties more used traditionally to discuss and rationalize the structure and reactivity of many organic and inorganic compounds [59]. A higher dipole moment will enhance inhibition efficiency due to large dipole–dipole interaction between the inhibitor molecule and the metal/alloy surface [60, 61]. The dipole moment of 8QSC is 9.6668 D. Generally, the low  $\Delta E$  and higher  $\mu$  gives better inhibition efficiency. Comparatively, the low  $\Delta E$  value and higher dipole moment of 8QSC gives better inhibition efficiency on the metal/alloy surface than

**Table 9** Quantum chemical parameters of 8QSC

$E_{\text{HOMO}}$ (eV)	$E_{\text{LUMO}}$ (eV)	$\Delta E$ (eV)	$\mu$ (D)	$E$ (Kcal/mol)	$I$	$A$	$\chi$ (eV)	$\eta$ (eV)	$\sigma$ (eV)
– 0.2665	– 0.1591	0.1074	9.6668	– 1409.776	0.2665	0.1591	0.2128	0.0537	18.62



(a)



(b)

**Fig. 13** DFT images of the investigated 8QSC: (a) HOMO structure of 8QSC and (b) LUMO structure of 8QSC

our previous studied NHQ inhibitor ( $\Delta E = 0.1328$  eV and  $\mu = 3.8163$  D) molecule [10]. The higher inhibition efficiency of 8QSC is further supported by the absolute reactivity parameter that is the lowest  $\eta$ , and higher  $\sigma$  value shown in Table 9. The calculated quantum chemical results were in good agreement with the experimental values. The higher inhibition efficiency of 8QSC is caused by the  $\text{SO}_2$  group attached to the quinoline ring. Also it contains a number of heteroatoms which play a major role in the adsorption process (Two ‘O,’ one N and one S).

## Conclusion

The surface protection of copper in 1.0 M  $\text{HNO}_3$  solution by 8QSC was studied using common electrochemical and surface morphological techniques. Theoretical and

adsorption study confirms the above electrochemical and surface technique results. According to experimental and theoretical findings, the principal conclusions are:

1. 8QSC is a good green corrosion inhibitor for copper metal in 1.0 M  $\text{HNO}_3$  solution. The inhibition efficiency increases with increase in inhibitor concentration.
2. The adsorption model obeys the Langmuir isotherm. The negative and lower value of the Gibbs free energy indicates 8QSC spontaneously and physically adsorbed on the copper surface.
3. In AC-IS measurements, the charge transfer resistance increase and double-layer capacitance decrease are characteristic of surface film formation.
4. The polarization curves show that 8QSC prevents hydrogen evolution reactions on the copper metal surface.
5. Further surface film formation confirm by SEM and AFM analysis.
6. Theoretical DFT calculation and FT-IR study confirm oxygen lone pair and protonated quinoline ring nitrogen help form a protective film on the copper metal surface.

**Conflict of interest** No conflict of interests regarding the publication of this paper.

## References

1. A. Zarrouk, B. Hammouti, A. Dafali, F. Bentiss, Inhibitive properties and adsorption of purpald as a corrosion inhibitor for copper in nitric acid medium. *J. Ind. Eng. Chem. Res.* **52**, 2560–2568 (2013)
2. A. Zarrouk, B. Hammouti, A. Dafali, H. Zarrok, R. Touzani, M. Bouacharine, M. Zertoubi, Inhibition of copper corrosion in acid solution by N-1-naphthylethylenediamine dihydrochloride momomethanolate: experimental and theoretical study: part-1. *Res. Chem. Intermed.* **38**, 1079–1089 (2012)
3. A.M. Eldesoky, M. Hassan, A.S. Fouda, Studies on the corrosion inhibition of copper in nitric acid solution using some pharmaceutical compounds. *Int. J. Electrochem. Sci.* **8**, 10376–10395 (2013)
4. K. Barouni, A. Kassale, A. Albourine, O. Jbara, B. Hammouti, L. Bazzi, Amino acids as corrosion inhibitors for copper in nitric acid medium: experimental and theoretical study. *J. Mater. Environ Sci.* **5**, 456–463 (2014)
5. H.L. Madkour, I.H. Elshamy, Experimental and computational studies on the inhibition performances of benzimidazole and its derivatives for the corrosion of copper in nitric acid. *Int. J. Ind. Chem.* **7**, 195–221 (2016)

6. K.F. Khaled, A. Fadl-Allah Sahar, B. Hammouti, Some benzotriazole derivatives as corrosion inhibitors for copper in acidic medium: Experimental and quantum chemical molecular dynamics approach. *Mat. Chem. Phys.* **117**, 148–155 (2009)
7. S.A. Abd El-Maksoud, H.H. Hassan, Electrochemical studies on the effect of (2E)-3- amino-2-phenylazo-but-2-enenitrile and its derivative on the behaviour of copper in nitric acid. *Mater. Corros.* **58**, 369–375 (2007)
8. A.S. Fouda, A. Abd El-Aal, A.B. Kandil, The effect of some phthalimide derivatives on corrosion behavior of copper in nitric acid. *Desalination* **201**, 216–223 (2006)
9. S. John, B. Joseph, K.V. Balakrishnan, K.K. Aravindakshan, A. Joseph, Electrochemical and quantum chemical study of 4-[(E)-(2,4-dihydroxy phenyl) methylidene] amino]-6-methyl-3-sulphanylidine-2,3,4,5-tetrahydro-1,2,4-triazin-5-one [DMSTT]. *Mater. Chem. Phys.* **123**, 218–224 (2010)
10. R. Ganapathi Sundaram, M. Sundaravadelu, Surface protection of mild steel in acidic chloride solution by 5-Nitro-8-Hydroxy Quinoline. *Egypt. J. Petrol.* (2017). <https://doi.org/10.1016/j.ejpe.2017.01.008>
11. S. John, R. Jeevana, K.K. Aravindakshan, A. Joseph, Corrosion inhibition of mild steel by N(4)-substituted thiosemicarbazone in hydrochloric acid media. *Egypt. J. Petrol.* (2016). <https://doi.org/10.1016/j.ejpe.2016.05.012>
12. R. Ganapathi Sundaram, M. Sundaravadelu, Anticorrosion activity of 8-quinoline sulphonyl chloride on mild steel in 1 M HCl solution. *J. Metal.* **1**, 1–9 (2016)
13. R. Ganapathi Sundaram, G. Vengatesh, M. Sundaravadelu, Effect of pharmaceutically active compound nitroxoline on the corrosion of mild steel in an acidic environment. *Adv. Chem.* **1**, 1–9 (2016)
14. A.Y. Musa, A.H. Kadhun, A.B. Mohamad, M.S. Takriff, Molecular dynamics and quantum chemical calculation studies on 4,4-dimethyl-3-thiosemicarbazide as corrosion inhibitor in 2.5 M H<sub>2</sub>SO<sub>4</sub>. *Mater. Chem. Phys.* **129**, 660–665 (2011)
15. A.S. Fouda, Y.M. Abdallah, G.Y. Elawady, R.M. Ahmed, Electrochemical study on the effectiveness of Hyoscyamus Muticus Extract as a green inhibitor for corrosion of copper in 1 M HNO<sub>3</sub>. *J. Mater. Environ. Sci.* **5**, 1519–1531 (2015)
16. R. Ganapathi Sundaram, G. Vengatesh, M. Sundaravadelu, Adsorption behavior and anti-corrosion capability of antibiotic drug Nitroxoline on copper in nitric acid medium. *J. Bio Tribo. Corros.* **3**, 1–13 (2017)
17. F. Bentiss, M. Traisnel, M. Lagrenee, The substituted 1, 3, 4-oxadiazoles: a new class of corrosion inhibitors of mild steel in acidic media. *Corros. Sci.* **42**, 127–146 (2000)
18. M.A. Quraishi, M.A.W. Khan, M. Ajmal, Influence of heterocyclic anils on corrosion inhibition and hydrogen permeation through mild steel in acid chloride environments. *Corrosion* **53**, 475–480 (1997)
19. E. Khamis, The effect of temperature on the acidic dissolution of steel in the presence of inhibitors. *Corrosion* **46**, 476–484 (1990)
20. A.K. Singh, M.A. Quraishi, The effect of some bis-thiadiazole derivatives on the corrosion of mild steel in hydrochloric acid. *Corros. Sci.* **52**, 1373–1385 (2010)
21. M. Revathi, K.K. Anupama, A. Joseph, Effect of methyl, ethyl and propyl substitution on benzimidazole for the protection of copper metal in nitric acid: theoretical and electrochemical screening studies. *J. Bio Tribo-Corros.* **3**, 1–15 (2017)
22. R. Ganapathi Sundaram, M. Sundaravadelu, Electrochemical and surface investigation of quinoline-8-sulphonyl chloride as corrosion inhibitor for mild steel in acidic medium. *Int. J. ChemTech Res.* **9**, 527–539 (2016)
23. R. Ganapathi Sundaram, M. Sundaravadelu, G. Karthik, G. Vengatesh, Inhibition effect of 4-hydroxyquinoline-2-carboxylic acid on corrosion of mild steel in 1 M sulphuric acid solution. *J. Chem. Pharm. Res.* **7**, 823–835 (2015)
24. M.K. Awad, M.R. Mustafa, M.M. Abo Elnga, Computational simulation of the molecular structure of some triazoles as inhibitors for the corrosion of metal surface. *J. Mol. Struct. (THEOCHEM)* **959**, 66–74 (2010)
25. H. Jiyaul, K.R. Ansari, V. Srivastava, M.A. Quraishi, I.B. Obot, Pyrimidine derivatives as novel acidizing corrosion inhibitors for N80 steel useful for petroleum industry: a combined experimental and theoretical approach. *J. Ind. Eng. Chem.* (2016). <https://doi.org/10.1016/j.jiec.2017.01.025>
26. M. Benahmed, I. Selatnia, A. Achouri, H. Laouer, N. Gherraf, S. Akkal, Steel corrosion inhibition by *Bupleurum Lancifolium* (Apiaceae) extract in acid solution. *Trans. Indian Inst. Met.* **68**, 393–401 (2015)
27. D.U. Omo-Dude, N.C. Oforika, Inhibition of the corrosion of mild steel in trioxonitrate (v) acid. *Niger. J. Phys.* **2**, 148–153 (1999)
28. P. Singh, E.E. Ebenso, L.O. Olasunkanmi, I.B. Obot, M.A. Quraishi, Electrochemical, theoretical and surface morphological studies of corrosion inhibition effect of green naphthyridine derivatives on mild steel in hydrochloric acid. *J. Phys. Chem.* **120**, 3408–3419 (2016)
29. Y. Sasikumar, A.S. Adekunle, L.O. Olasunkanmi, I. Bahadur, R. Baskar, M.M. Kabanda, I.B. Obot, E.E. Ebenso, Electrochemical, quantum chemical and Monte Carlo simulation studies on the corrosion inhibition of some alkyl imidazolium ionic liquids containing tetrafluoroborate anion on mild steel in acidic medium. *J. Mol. Liq.* **211**, 105–118 (2015)
30. S.A. Umoren, I.B. Obot, A.U. Israel, P.O. Asuquo, M.M. Solomon, U.M. Eduok, A.P. Udoh, Inhibition of mild steel corrosion in acidic medium using coconut coir dust extracted from water and methanol as solvents. *J. Ind. Eng. Chem.* **20**, 3612–3622 (2014)
31. R. Ganapathi Sundaram, G. Karthik, G. Vengatesh, M. Sundaravadelu, Adsorption characteristics of Kynurenic acid as corrosion inhibitor at mild steel/hydrochloric acid interface. *Der Chem. Sin.* **6**, 54–63 (2015)
32. X. Xu, A. Singh, Z. Sun, K.R. Ansari, Y. Lin, Theoretical, thermodynamic and electrochemical analysis of biotin drug as an impending corrosion inhibitor for mild steel in 15% hydrochloric acid. *R. Soc. Open sci.* (2017). <https://doi.org/10.1098/rsos.170933>
33. S.M. Tawfik, Alginate surfactant derivatives as an ecofriendly corrosion inhibitor for carbon steel in acidic environments. *RSC Adv.* **5**, 104535–104550 (2015)
34. H.S. Gadow, M.M. Motawea, Investigation of the corrosion inhibition of carbon steel in hydrochloric acid solution by using ginger roots extract. *RSC Adv.* **7**, 24576–24588 (2017)
35. M. Lebrini, M. Lagrenee, H. Vezin, M. Traisnel, F. Bentiss, Experimental and theoretical study for corrosion inhibition of mild steel in normal hydrochloric acid solution by some new macrocyclic polyether compounds. *Corros. Sci.* **49**, 2254–2269 (2007)
36. P. Bommersbach, C. Alamy-Ddmont, J.P. Millet, B. Normand, Hydrodynamic effect on the behaviour of a corrosion inhibitor film: characterization by electrochemical impedance spectroscopy. *Electrochem. Acta.* **51**, 4011–4018 (2006)
37. A.K. Singh, M.A. Quraishi, Effect of 2,2' benzothiazolyl disulfide on the corrosion of mild steel in acid media. *Corros. Sci.* **51**, 2752–2760 (2009)
38. A. Singh, Y. Lin, I.B. Obot, E.E. Ebenso, K.R. Ansari, M.A. Quraishi, Corrosion mitigation of J55 steel in 3.5% NaCl solution by a macrocyclic inhibitor. *Appl. Surf. Sci.* **356**, 341–347 (2015)
39. B.M. Prasanna, B.M. Praveen, N. Hebbar, T.V. Venkatesha, H.C. Tandan, Inhibition study of mild steel corrosion in 1 M

- hydrochloric acid solution by 2-chloro 3-formyl quinoline. *Int. J. Indus. Chem.* **7**, 9–19 (2016)
40. M. Mobin, S. Masroor, Cationic gemini surfactants as novel corrosion inhibitor for mild steel in 1 M HCl. *Int. J. Electrochem. Sci.* **7**, 6920–6940 (2012)
  41. M. Mahdavian, S. Ashhari, Corrosion inhibition performance of 2-mercaptobenzimidazole and 2-mercaptobenzoxazole compounds for protection of mild steel in hydrochloric acid solution. *Electrochim. Acta* **55**, 1720–1724 (2010)
  42. M. Tourabi, K. Nohair, M. Traisnel, C. Jama, F. Bentiss, Electrochemical and XPS studies of the corrosion inhibition of carbon steel in hydrochloric acid pickling solutions by 3,5-bis(2-thienyl methyl)-4-amino-1,2,4-triazole. *Corros. Sci.* **75**, 123–133 (2013)
  43. A.Y. Musa, A.A.H. Kadhum, A.B. Mohamad, M.S. Takriff, Experimental and theoretical study on the inhibition performance of triazole compounds for mild steel corrosion. *Corros. Sci.* **52**, 3331–3340 (2010)
  44. E.S. Ferreira, C. Giancomelli, F.C. Giancomelli, A. Spinelli, Evaluation of the inhibitor effect of L-ascorbic acid on the corrosion of mild steel. *Mater. Chem. Phys.* **83**, 129–134 (2004)
  45. W.-H. Li, Q. He, S.-T. Zhang, C.I. Pei, B.-R. Hou, Some new triazole derivatives as inhibitors for mild steel corrosion in acidic medium. *J. Appl. Electrochem.* **38**, 289–295 (2008)
  46. D.K. Yadav, M.A. Quraishi, B. Maiti, Inhibition effect of some benzylidenes on mild steel in 1 M HCl: an experimental and theoretical correlation. *Corros. Sci.* **55**, 254–266 (2012)
  47. K.R. Ansari, M.A. Quraishi, E. Ebenso, Electrochemical and thermodynamic investigation of diclofenac sodium drug as a potential corrosion inhibitor for mild steel in hydrochloric acid. *Int. J. Electrochem. Sci.* **8**, 12860–12873 (2013)
  48. K. Barouni, A. Kassale, L. Bazzi, R. Salghi, B. Hammouti, A. Albourine, S. El Issami, O. Jbara, M. Bouachrine, Inhibition of corrosion of copper in nitric acid solution by four amino acids. *Res. Chem. Intermed.* **40**, 991–1002 (2014)
  49. C. Verma, M.A. Quraishi, E.E. Ebenso, I.B. Obot, A. El-Assyry, 3-Amino alkylated indoles as corrosion inhibitors for mild steel in 1 M HCl: experimental and theoretical studies. *J. Mol. Liq.* **219**, 647–660 (2016)
  50. P.A. Tarantilis, V.E. Troianou, C.S. Pappas, Y.S. Kotseridis, M.G. Polissiou, Differentiation of Greek red wines on the basis of grape variety using attenuated total reflectance Fourier transform infrared spectroscopy. *Food Chem.* **111**, 192–196 (2008)
  51. A.P. Srikanth, T.G. Sunitha, V. Raman, S. Nanjundan, N. Rajendran, Effect of benzotriazole derivatives on the corrosion of brass in NaCl solutions. *Mater. Chem. Phys.* **103**, 241–247 (2007)
  52. S. Jyothi, J. Ravichandran, Corrosion inhibition of mild steel in sulphuric acid using *Luffa Aegyptiaca* leaves extract. *Acta Metall. Sin. (Engl. Lett.)* **27**, 969–980 (2014)
  53. R.M. Issa, M.K. Awad, F.M. Atlam, DFT theoretical studies of antipyrine Schiff bases as corrosion inhibitors. *Mater. Corros.* **61**, 709–714 (2010)
  54. N.O. Obi-Egbedi, I.B. Obot, M.I. El-Khaiary, Quantum chemical investigation and statistical analysis of the relationship between corrosion inhibition efficiency and molecular structure of xanthene and its derivatives on mild steel in sulphuric acid. *J. Mol. Struct.* **1002**, 86–96 (2011)
  55. S. Hari Kumar, S. Karthikeyan, Torsemide and furosemide as green inhibitors for the corrosion of mild steel in hydrochloric acid medium. *Ind. Eng. Chem. Res.* **52**, 7457–7469 (2013)
  56. N. Hackerman, E.S. Snively Jr., J.S. Payne Jr., Effects of anions on corrosion inhibition by organic compounds. *J. Appl. Electrochem.* **113**, 677–681 (1966)
  57. R. Hasanov, S. Bilge, S. Bilgic, G. Gece, Z. Kilic, Experimental and theoretical calculations on corrosion inhibition of steel in 1 M H<sub>2</sub>SO<sub>4</sub> by crown type polyethers. *Corros. Sci.* **52**, 984–990 (2010)
  58. C. Oğretir, B. Mihci, G. Bereket, Quantum chemical studies of some pyridine derivatives as corrosion inhibitors. *J. Mol. Struct.* **488**, 223–231 (1999)
  59. V.S. Saatri, *Corrosion inhibitors: principles and applications* (Wiley, Chichester, 1998)
  60. S.T. Arab, Inhibition action of thiosemicabazone and some of its *p*-substituted compounds on the corrosion of iron-base metallic glass alloy in 0.5 M H<sub>2</sub>SO<sub>4</sub> at 30 °C. *Mater. Res. Bull.* **43**, 510–521 (2008)
  61. N. Soltani, M. Behpour, E.E. Oguzie, M. Matiluji, M.A. Ghasemzadeh, Pyrimidine-2-thione derivatives as corrosion inhibitors for mild steel in acidic environments. *RSC Adv.* **5**, 11145–11162 (2015)